Central dilepton production via photon-photon fusion in proton-proton collisions with one forward proton

A. Szczurek^{1,2}, B. Linek and M. Luszczak

¹ The Henryk Niewodniczański Institute of Nuclear Physics Polish Academy of Sciences ²University of Rzeszów

Krakow, April 23 2021

Contents

- Introduction
- Sketch of the formalism
- Inclusive production
 (integrated cross section, distributions, structure functions,)
- Cut on ξ variable(s)
 (integrated cross section, distributions, structure functions,)
- ▶ Range of x_{Bj} and/or Q^2 tested in the $pp \rightarrow I^+I^-(p)$ processes
- (Mini)jet or final state emissions
- SuperChic results (distributions, differential gap survival factor)
- Conclusions and outlook



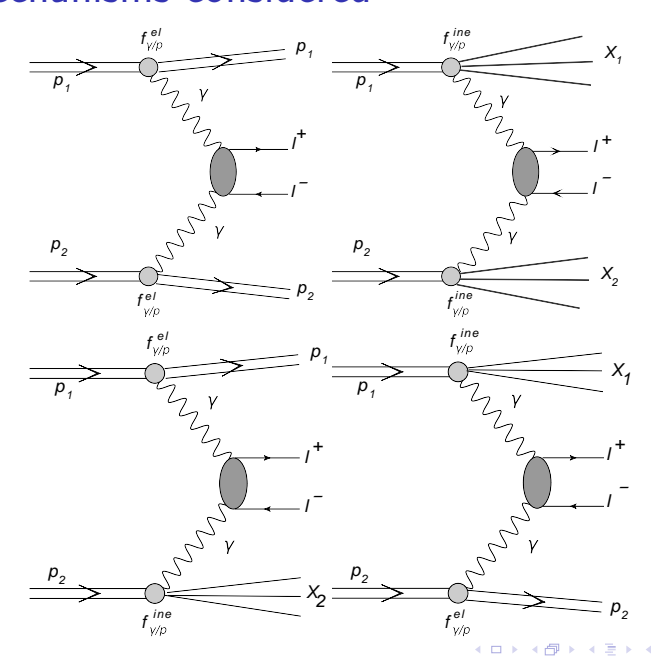
Introduction

- We wish to discuss production of dilepton pairs in proton-proton collisions via photon-photon fusion including photon transverse momenta.
- Both ATLAS and CMS performed relevant measurements (without and with proton measurements)
- ► Here we concentrate on the case with one forward proton (CMS (poor statistics), ATLAS (better statistics, 14.6 fb⁻¹, both e^+e^- and $\mu^+\mu^-$).
- Our group was the first which proposed to use the formalism with photon transverse momenta.
- ▶ The same formalism can be also used for production of W^+W^- and $t\bar{t}$ pairs.
- ► Here we wish to discuss consequences of proton measurement for the cross section, differential distributions, gap survival factor, etc.
- We will also use the popular SuperChic-4 generator where the same formalism was implemented. It also includes kinemtics-dependent soft gap survival factor as developed by the Durham group.

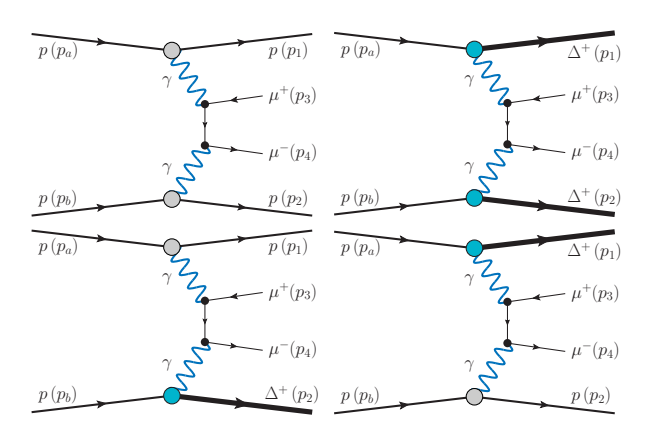
Our previous papers on the subject

- ▶ G.G. da Silveira, L. Forthomme, K. Piotrzkowski, W. Schäfer and A. Szczurek, Ćentral $\mu^+\mu^-$ production via photon-photon fusion in proton-proton collisions with proton dissociation", JHEP **02** (2015) 159.
- M. Luszczak, W. Schäfer and A. Szczurek, "Two-photon dilepton production in proton-proton collisions: Two alternative approaches", Phys. Rev. D93 (2016) 074018.
- ▶ M. Luszczak, W. Schäfer and A. Szczurek, "Production of W^+W^- pairs via $\gamma^*\gamma^*\to W^+W^-$ subprocess with photon transverse momenta", JHEP05 (2018) 064.
- P. Lebiedowicz and A. Szczurek, "Exclusive and semiexclusive production of $\mu^+\mu^-$ pairs with Delta isobars and other resonances in the final state and the size of absorption effects", Phys. Rev. **D98** (2018) 053007.
- L. Forthomme, M. Luszczak, W. Schäfer and A. Szczurek, "Rapidity gap survival factors caused by remnant fragmentation for W^+W^- pair production via $\gamma^*\gamma^* \to W^+W^-$ subprocess with photon transverse momenta", Phys. Lett. **B789** (2019) 300.
- M. Luszczak, L. Forthomme, W. Schäfer and A. Szczurek, "Production of $t\bar{t}$ pairs via $\gamma\gamma$ fusion with photon transverse momenta and proton dissociation", JHEP **02** (2019) 100.

The mechanisms considered



Resonance production



Rysunek: Four different categories of $\gamma\gamma$ fusion mechanisms of dilepton production in proton-proton collisions with resonances in the final state.

Sketch of the formalism

In the k_T -factorization approach, the cross section for I^+I^- production can be written in the form

$$\frac{d\sigma^{(i,j)}}{dy_1 dy_2 d^2 \boldsymbol{p}_1 d^2 \boldsymbol{p}_2} = \int \frac{d^2 \boldsymbol{q}_1}{\pi \boldsymbol{q}_1^2} \frac{d^2 \boldsymbol{q}_2}{\pi \boldsymbol{q}_2^2} \mathcal{F}_{\gamma^*/A}^{(i)}(x_1, \boldsymbol{q}_1) \mathcal{F}_{\gamma^*/B}^{(j)}(x_2, \boldsymbol{q}_2) \frac{d\sigma^*(\boldsymbol{p}_1, \boldsymbol{p}_2; \boldsymbol{q}_1, \boldsymbol{q}_2)}{dy_1 dy_2 d^2 \boldsymbol{p}_1 d^2 \boldsymbol{p}_2},$$

$$\tag{1}$$

where the indices $i, j \in \{el, in\}$ denote elastic or inelastic final states.

Here the photon flux for inelatic case is integrated over the mass of the remnant.

Sketch of the formalism

The longitudinal momentum fractions of photons are obtained from the rapidities and transverse momenta of final state I^+I^- as:

$$x_{1} = \sqrt{\frac{\boldsymbol{p}_{1}^{2} + m_{I}^{2}}{s}} e^{+y_{1}} + \sqrt{\frac{\boldsymbol{p}_{2}^{2} + m_{I}^{2}}{s}} e^{+y_{2}} ,$$

$$x_{2} = \sqrt{\frac{\boldsymbol{p}_{1}^{2} + m_{I}^{2}}{s}} e^{-y_{1}} + \sqrt{\frac{\boldsymbol{p}_{2}^{2} + m_{I}^{2}}{s}} e^{-y_{2}} .$$
(2)

Four-momenta of intermediate photons:

$$q_1 \approx \left(x_1 \frac{\sqrt{s}}{2}, \vec{q}_{1t}, x_1 \frac{\sqrt{s}}{2}\right),$$
 $q_2 \approx \left(x_2 \frac{\sqrt{s}}{2}, \vec{q}_{2t}, -x_2 \frac{\sqrt{s}}{2}\right).$ (3)

Photon fluxes

The integrated fluxes for elastic and inelastic processes can be found in our published papers (see also Budneev, Ginzburg, Serbo et al.)

- ▶ The elastic flux is expressed via proton electromagnetic form factors.
- The inelastic flux is expressed via proton structure function (F_2 and F_L).

If one is interested in modeling what happens with the proton remnant than the formalism must be extended. Then the unintegrated inelastic photon distribution (flux) can be written as:

$$\mathcal{F}_{ine}(x, q_t^2) = \int dM^2 \frac{d\mathcal{F}_{ine}}{dM^2} (x, q_t^2, M^2) , \qquad (4)$$

where $\frac{d\mathcal{F}_{ine}}{dM^2}(x,q_t^2,M^2)$ is a more differential photon distribution in the proton. We shall call it *doubly-unintegrated* photon distribution (flux).

The latter distribution was used to calculate differential distributions for production of W^+W^- (FLSS2019) or $t\bar{t}$ (LFSS2019) pairs with rapidity gap at midrapidities.

Photon fluxes

Inelastic flux:

$$\mathcal{F}_{\gamma^* \leftarrow A}^{\text{in}}(z, q) = \frac{\alpha_{\text{em}}}{\pi} \left\{ (1 - z) \left(\frac{q^2}{q^2 + z(M_X^2 - m_\rho^2) + z^2 m_\rho^2} \right)^2 \frac{F_2(x_{\text{Bj}}, Q^2)}{Q^2 + M_X^2 - m_\rho^2} \right. \\ + \frac{z^2}{4x_{\text{Bj}}^2} \frac{q^2}{q^2 + z(M_X^2 - m_\rho^2) + z^2 m_\rho^2} \frac{2x_{\text{Bj}} F_1(x_{\text{Bj}}, Q^2)}{Q^2 + M_X^2 - m_\rho^2} \right\},$$
 (5)

Ingredients: F_1 and F_2 structure functions

Elastic flux:

$$\begin{split} \mathcal{F}_{\gamma^* \leftarrow A}^{\mathrm{el}}(z,q) &= \frac{1}{\pi} \left\{ (1-z) \left(\frac{q^2}{q^2 + z(M_X^2 - m_\rho^2) + z^2 m_\rho^2} \right)^2 \frac{4 m_\rho^2 \, G_E^2(Q^2) + Q^2 \, G_M^2(Q^2)}{4 m_\rho^2 + Q^2} \right. \\ &+ \frac{z^2}{4} \frac{q^2}{q^2 + z(M_X^2 - m_\rho^2) + z^2 m_\rho^2} \, G_M^2(Q^2) \right\} \, . \end{split}$$

(6)

Ingredients: Electromagnetic form factors

V. M. Budnev, I. F. Ginzburg, G. V. Meledin and V. G. Serbo, Phys. Rept. **15**, 181 (1975).

Parametrizations of structure functions of proton

ALLM parametrization

► H. Abramowicz, E. M. Levin, A. Levy and U. Maor Phys. Lett. **B269**, (1991) 465

$$F_2(x, Q^2) = \frac{Q^2}{Q^2 + m_0^2} \left(F_2^{\mathcal{P}}(x, Q^2) + F_2^{\mathcal{R}}(x, Q^2) \right)$$

FFJLM parametrization

R. Fiore, A. Flachi, L. L. Jenkovszky, A. I. Lengyel and V. K. Magas - Phys. Rev. D70, 054003 (2004)

$$\mathcal{I}mlpha(s) = s^{\delta} \sum_{n} c_{n} \left(\frac{s - s_{n}}{s} \right)^{\mathcal{R}elpha(s_{n})} \cdot \theta(s - s_{n})$$
 $\mathcal{R}e\,lpha(s) = lpha(0) + rac{s}{\pi} PV \int_{0}^{\infty} ds' rac{\mathcal{I}mlpha(s')}{s'(s' - s)}$



Parametrizations of structure functions of proton

SU parametrization

A. Szczurek, V. Uleshchenko
 Eur. Phys. J. C12 (2000) 663-671

$$F_2^N(x, Q^2) = F_2^{N,VDM}(x, Q^2) + F_2^{N,part}(x, Q^2)$$

$$F_2^{N,VDM}(x,Q^2) = \frac{Q^2}{\pi} \sum_V \frac{M_V^4 \cdot \sigma_{VN}^{tot}(s^{1/2})}{\gamma_V^2 (Q^2 + M_V^2)^2} \cdot \Omega_V(x,Q^2)$$

$$F_2^{N,part}(x,Q^2) = rac{Q^2}{Q^2 + Q_0^2} \cdot F_2^{asymp}(ar{x},ar{Q}^2)$$

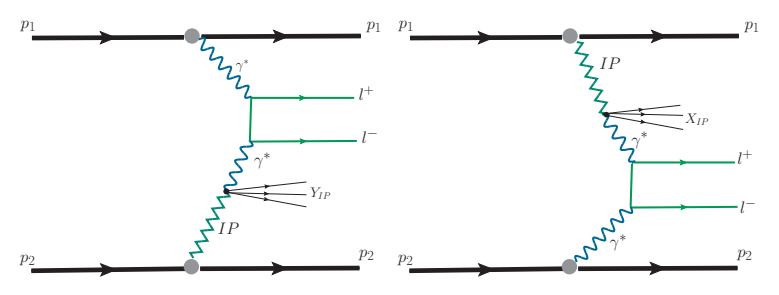


LUX-like structure function

a newly constructed parametrization, which at $Q^2 > 9 \,\mathrm{GeV}^2$ uses an NNLO calculation of F_2 and F_L from NNLO MSTW 2008 partons. It employs a useful code by the MSTW group to calculate structure functions. At $Q^2 < 9 \,\mathrm{GeV}^2$ this fit uses the parametrization of Bosted and Christy in the resonance region, and a version of the ALLM fit published by the HERMES Collaboration for the continuum region. It also uses information on the longitudinal structure function from SLAC. As the fit is constructed closely following LUX QED work we call this fit LUX-like.

Proton from remnants

In principle, proton can be emitted also from the the remnant system. This requires modelling of remnant fragmentation which is not fully under control. Such protons carry typically much reduced longitudinal momentum fraction $x_{p,i}$ such that $\xi_i = 1 - x_{p,i} > 0.1$, i.e. cannot be measured in the Roman pots of the ATLAS or CMS experiments.



Rysunek: Diffractive mechanisms of dilepton production in proton-proton collisions.

Diffractive processes

Only the diffractive mechanism shown in the previous slide could lead to $\xi_i < 0.1$. However, the diffractive mechanism happens only in about 10 % of all cases as was measured at HERA. In addition the pomeron remnant would destroy the rapidity gap. Such a process was not discussed in the context of I^+I^- production in p p collisions with rapidity gap requirement. Also the diffractive photon distribution in pomeron was not discussed. One may expect:

$$\frac{d\mathcal{F}_{diff}}{dM^2}(x, q_t^2, M^2) \ll \frac{d\mathcal{F}_{ine}}{dM^2}(x, q_t^2, M^2) . \tag{7}$$

In addition, the pomeron remnant would destroy the rapidity gap and the rapidity gap veto would almost totally eliminate contribution of such processes in the context of forward proton measurement discussed in the present paper.

Arguments of structure functions

Calculated from photon transverse momentum and mass of the remnant.

Bjorken-x:

$$x_{Bj1} = \frac{Q_1^2}{Q_1^2 + M_X^2 - m_p^2},$$

 $x_{Bj2} = \frac{Q_2^2}{Q_2^2 + M_Y^2 - m_p^2}.$

Photon virtuality:

$$Q_1^2 \approx q_{1t}^2$$
,
 $Q_2^2 \approx q_{2t}^2$.

Forward proton

The ATLAS collaboration analysis impose the consistency requirements:

$$\xi_1 = \xi_{\parallel}^+ , \ \xi_2 = \xi_{\parallel}^- .$$
 (8)

The longitudinal momentum fractions of the photons were calculated in the ATLAS analysis as:

$$\xi_{II}^{+} = \left(M_{II}/\sqrt{s}\right) \exp(+Y_{II}) ,$$

$$\xi_{II}^{-} = \left(M_{II}/\sqrt{s}\right) \exp(-Y_{II}) .$$
 (9)

Only lepton variables enter the formula. We will use the same formula in our analysis.

Integration parameters

Multiple integration (Vegas method):

$$q_{1t}, q_{2t}, \phi_1, \phi_2, y_1, y_2, p_{t,diff}, \phi_{p_{t,diff}}$$
 and M_X or M_Y .

9 or 10 integration variables.

Many interesting correlations between variables.

Careful adjustment of ranges of some integration parameters is required.

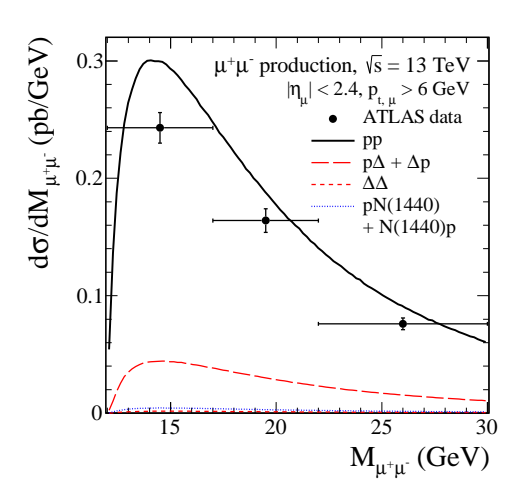
$$q_{1t},\,q_{2t}<100$$
 - 500 GeV, $\textit{M}_{\textit{X}},\,\textit{M}_{\textit{Y}}<500$ - 1000 GeV.

This depends on experimental cuts and acceptances.

Summary of our programs

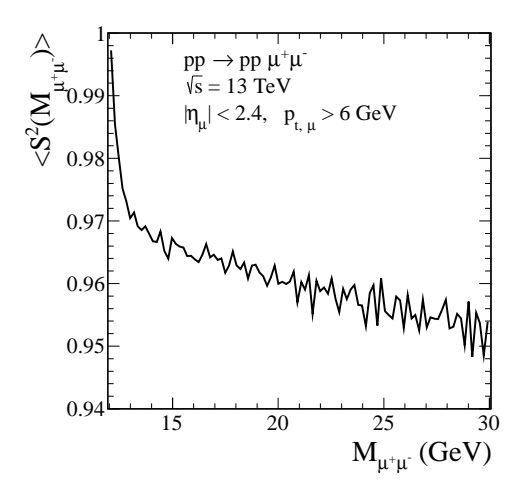
We have 3 different versions of our codes:

- ► (a) calculate differential distributions using single unintegrated photon distributions
- ▶ (b) calculate differential distributions using doubly unintegrated photon distributions
- (c) generator version generates unweighted events.
 Distributions done in an additional program or using Root program.

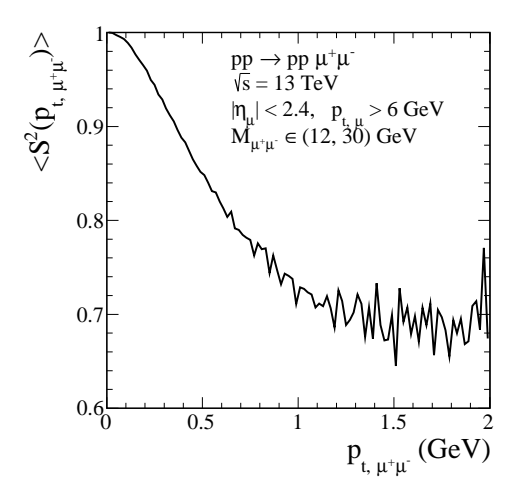


Rysunek: Dimuon invariant mass distribution without proton measurement and the ATLAS data.

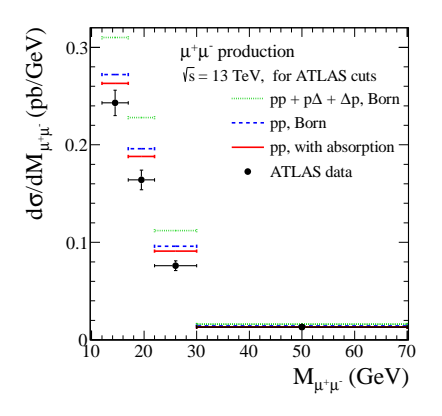
 $p_{t,\mu} > 6$ GeV, $p_{t,pair} < 1.5$ GeV, $-2.4 < y_1, y_2 < 2.4$, rapidity gap ~ 9.9



Rysunek: Gap survival factor for dimuon invariant mass distribution without proton measurement.



Rysunek: Soft gap survival factor as a function of $p_{t,pair}$.



Rysunek: The differential cross sections $d\sigma/dM_{\mu^+\mu^-}$ for the $\mu^+\mu^-$ production at $\sqrt{s}=13$ TeV with the ATLAS experimental cuts. Our "exact $2\to 4$ kinematics" predictions (lines) are compared with the ATLAS differential fiducial cross sections.

Results of the new analysis

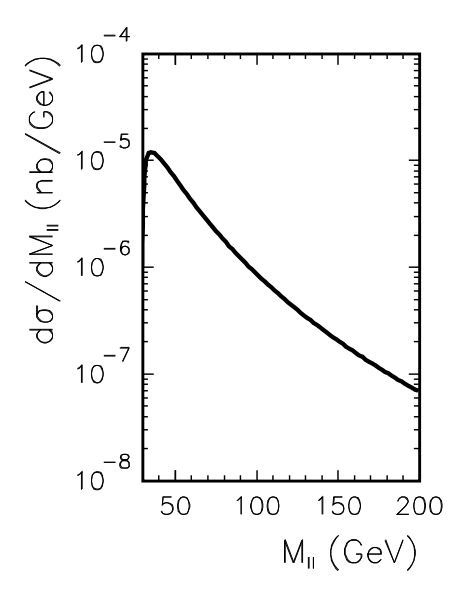
In the calculations described below we shall take typical cuts on dileptons:

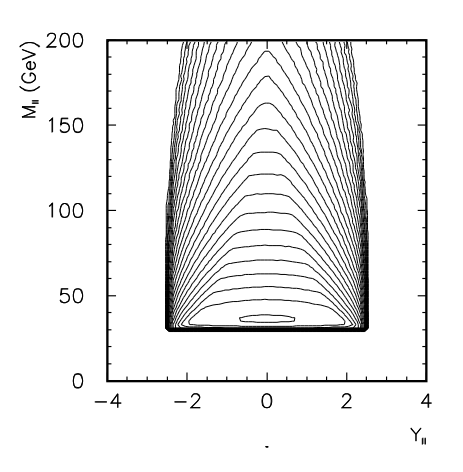
- \triangleright -2.5 < y_1, y_2 < 2.5
- ▶ $p_{1t}, p_{2t} > 15 \text{ GeV}$

We shall show also results with extra cuts on ξ_{\parallel}^+ or ξ_{\parallel}^- .

In the following we do not exclude:

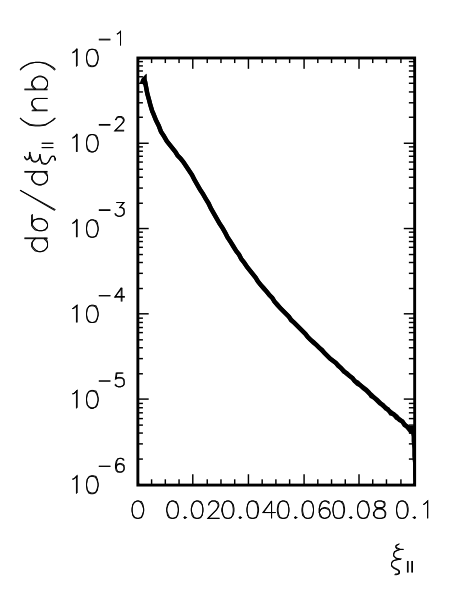
- ▶ mass window arround Z-boson mass m_Z , as was done in (ATLAS).
- ► cut on lepton acoplanarity

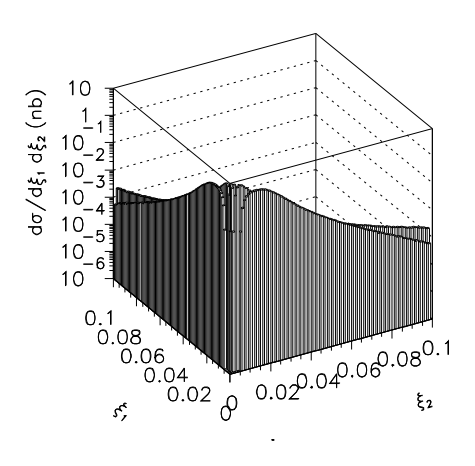




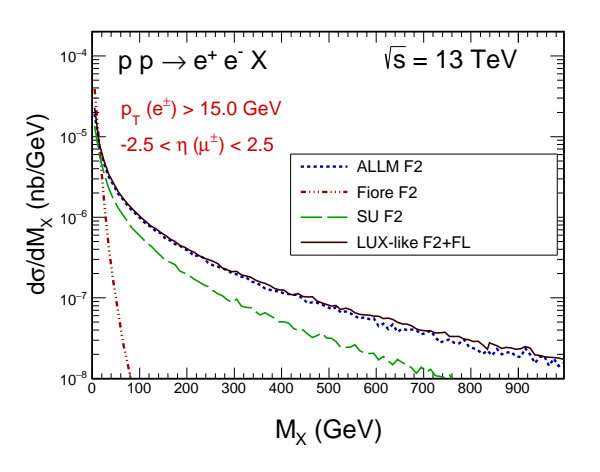
Rysunek: Here no cuts on neither ξ_1 nor ξ_2 were imposed. The $p_{t,\mu}>15$ GeV condition was imposed here.



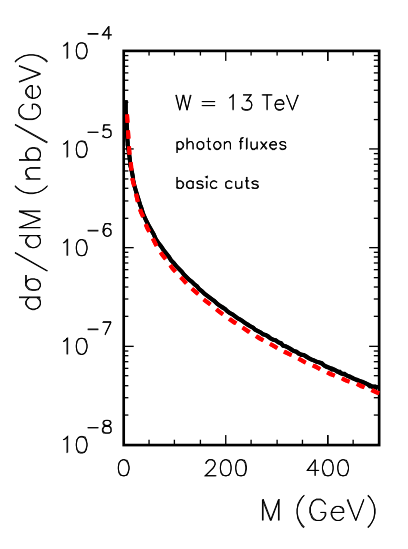




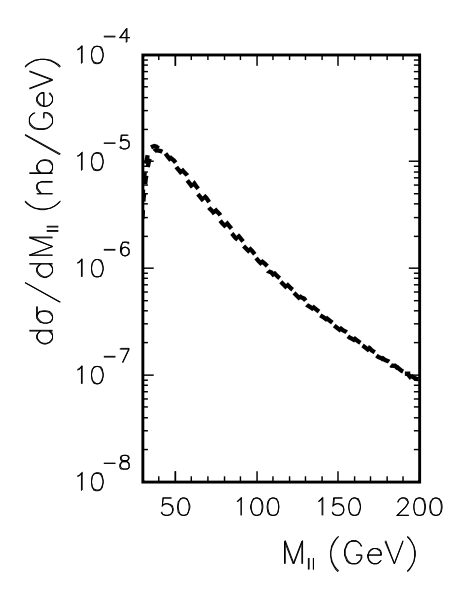
Rysunek: Two-dimensional distribution in $(\xi_{\parallel}^+, \xi_{\parallel}^-)$ for the double-elastic mechanism.

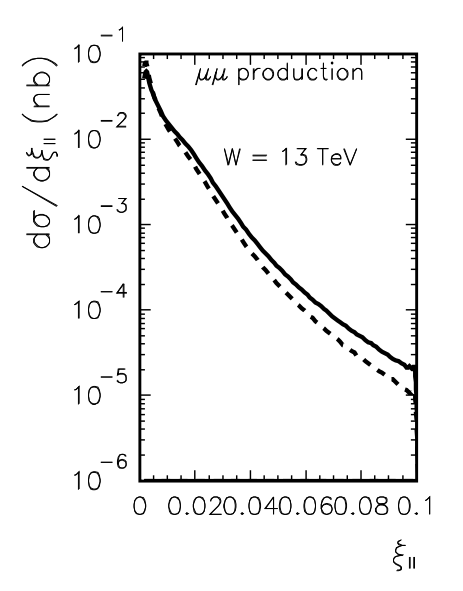


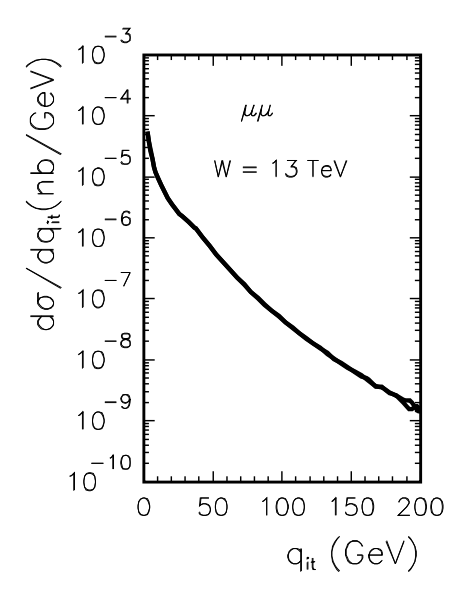
Rysunek: Distribution in the mass of the baryonic remnant system $(M_X \text{ or } M_Y)$ for different structure functions from the literature. In the case of SU parametrization only partonic contribution is included.

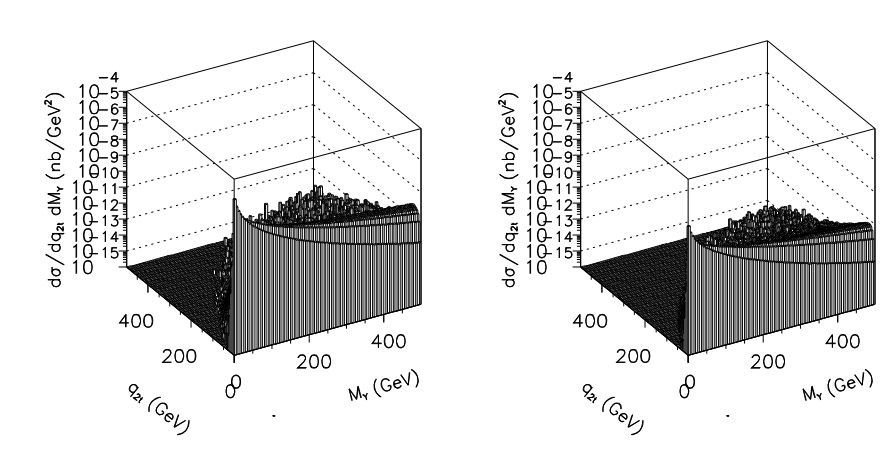


Rysunek: Distribution in the mass of the baryonic remnant system $(M_X \text{ or } M_Y)$ for ALLM (black solid) and Szczurek (red dashed)



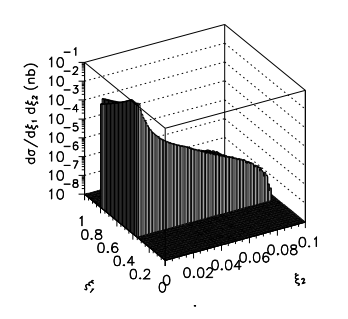


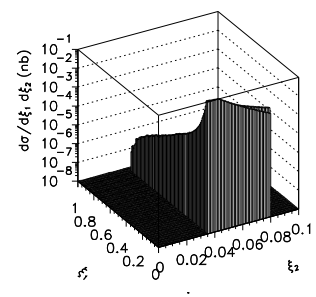


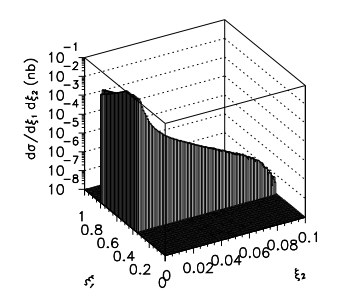


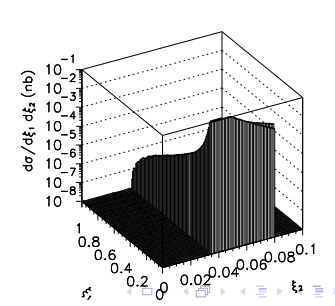
Rysunek: Two-dimensional distribution in (q_{2t}, M_Y) for elastic-inelastic contribution. We show results without ξ cut (left panel) and with ξ cut (right panel).

ξ_{\parallel}^{+} or ξ_{\parallel}^{-} cuts







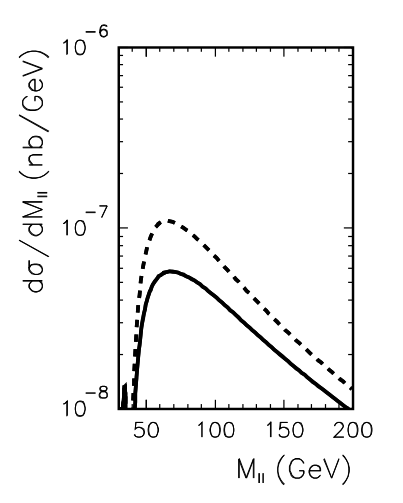


$\xi_{\rm I\hspace{-.1em}I\hspace{-.1em}I}^+$ or $\xi_{\rm I\hspace{-.1em}I\hspace{-.1em}I}^-$ cuts

Tablica: Integrated cross section for $\mu^+\mu^-$ with one p in 0.035 $<\xi_{||}^{\pm}<$ 0.08. Here $p_{1t},p_{2t}>$ 15 GeV and -2.5 < $y_1,y_2<$ 2.5. In the paranthesis result with $p_{t,sum}<$ 5 GeV. 2UN – doubly unintegrated photon distribution and GEN – generator version.

| contribution | c.s. in fb without ξ -cuts | c.s. in fb with ξ -cuts |
|--|--------------------------------|-----------------------------|
| elastic-elastic, cut on proton 1 | 358.68 | 5.4591 |
| elastic-elastic, cut on proton 2 | | 5.4592 |
| elastic-inelastic, cut on proton 1, SU, 0-100 GeV | 427.8949 | 10.0190 (3.3492) |
| inelastic-elastic, cut on proton 2 SU, 0-100 GeV | 427.0130 | 10.0186 (3.3491) |
| elastic-inelastic, VDM (no Ω), 0-100 GeV | 98.0215 (2UN) | |
| inelastic-elastic, VDM (no Ω), 0-100 GeV | 98.0297 (2UN) | |
| elastic-inelastic SU partonic | 449.1076 (2UN) | |
| inelastic-elastic SU partonic | 449.0985 (2UN) | |
| elastic-inelastic, cut on proton 1, ALLM | 468.6102 (2UN) | 11.8292 |
| inelastic-elastic, cut on proton 2, ALLM | 468.6102 (2UN) | 11.8294 |
| elastic-inelastic, new Szczurek | 461.5330 (2UN) | 12.6046 [14.1823] (5.9311) |
| inelastic-elastic, new Szczurek | 461.5750 (2UN) | 12.6032 [14.1806] (5.9309) |
| elastic-inelastic, ALLM | 571.871 (GEN) | 9.711 |
| inelastic-elastic, ALLM | 571.562 (GEN) | 9.621 |
| elastic-inelastic, LUX-like, $F_2 + F_1$ | 635.215 (GEN) | 19.894 |
| inelastic-elastic, LUX-like, $F_2 + F_1$ | 635.102 (GEN) | 19.831 |
| elastic-inelastic, LUX-like, $\overline{F_2}$ only | (GEN) | |
| inelastic-elastic, LUX-like, F_2 only | 656.702 (GEN) | |
| elastic-inelastic, cut on proton 1, resonances | 38.6709 (2UN) | 0.57872 |
| inelastic-elastic, cut on proton 2 resonances | 38.6639 (2UN) | 0.57872 |
| elastic-inelastic, cut on proton 1, Δ^+ | 28.5844 (2UN) | 0.42755 |
| inelastic-elastic, cut on proton 2 Δ^+ | 28.5814 (2UN) | 0.42763 |

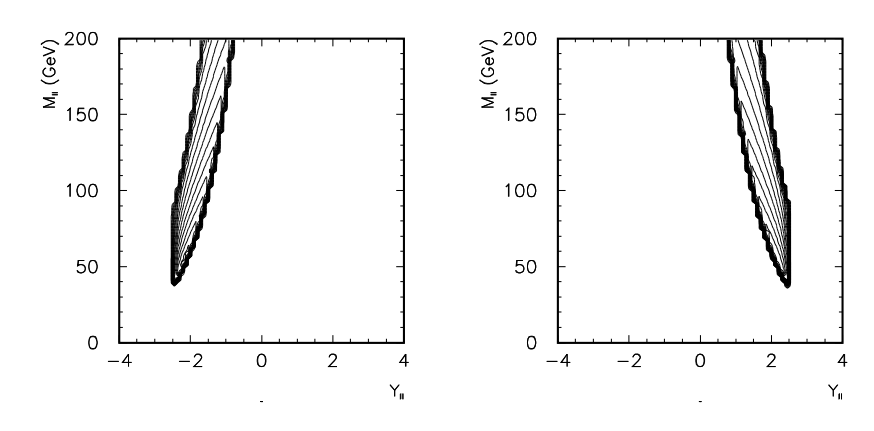




Rysunek: Distribution in dilepton invariant mass for four different contributions considered.

Here the cuts on ξ_{\parallel}^{+} or ξ_{\parallel}^{-} are imposed. The solid line is for double electic contribution and the dashed line is for single dissociation.

ξ -cut, double-elastic contribution

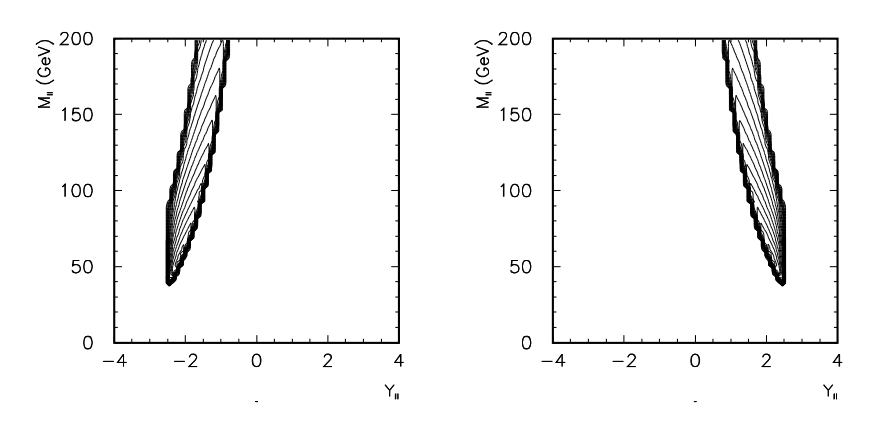


Rysunek: Here we have imposed experimental condition for ξ_2 (left panel) or ξ_1 (right panel).

The $p_{t,\mu} > 15$ GeV condition was imposed in addition.

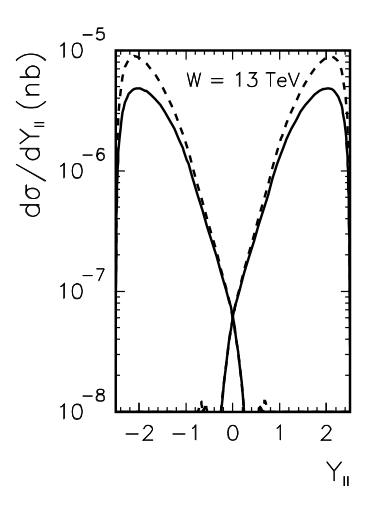


ξ -cut, single-dissociative contribution

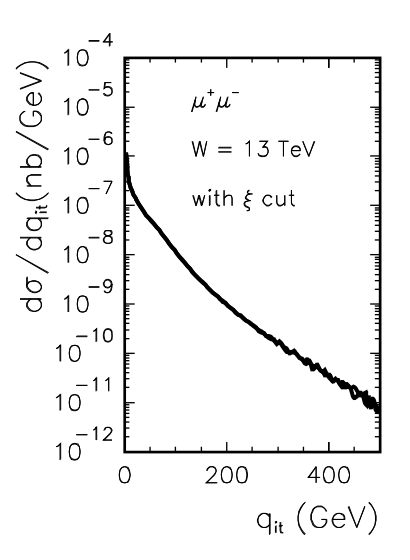


Rysunek: Here we have imposed experimental condition on ξ_1 (left panel) or ξ_2 (right panel).

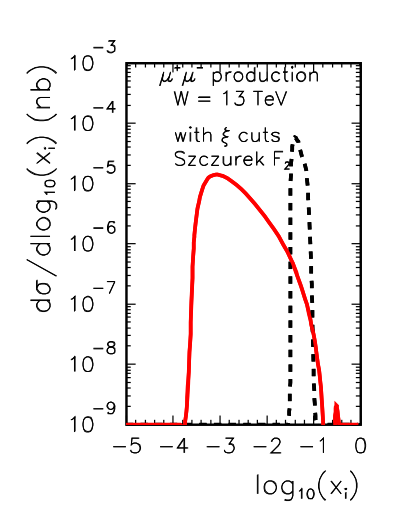
Szczurek-Uleshchenko structure function parametrization was used here. The $p_{t,u} > 15$ GeV condition has been imposed in addition.

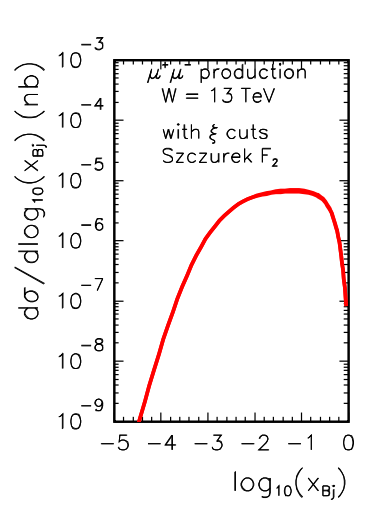


Rysunek: Here the cuts on ξ_{II}^+ or ξ_{II}^- are imposed. The solid line is for double elastic contribution and the dashed line is for single dissociation contribution.

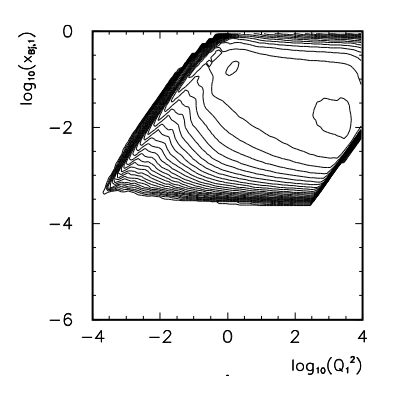


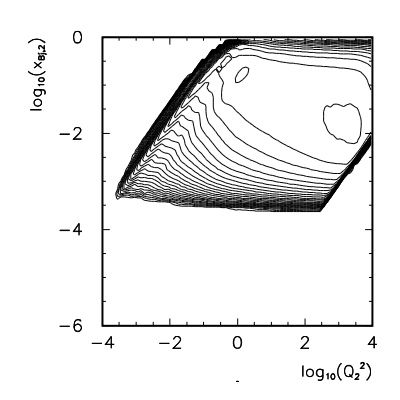
Rysunek: Distribution in q_{it} . Here the cuts on $\xi_{||}^+$ or $\xi_{||}^-$ are imposed.





Arguments of the structure functions

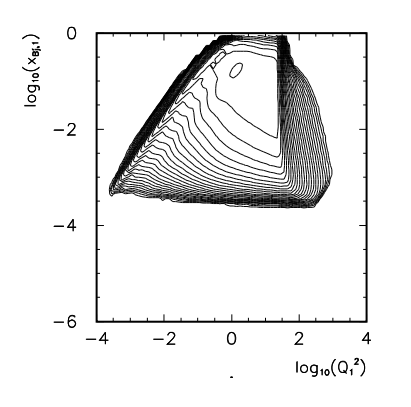


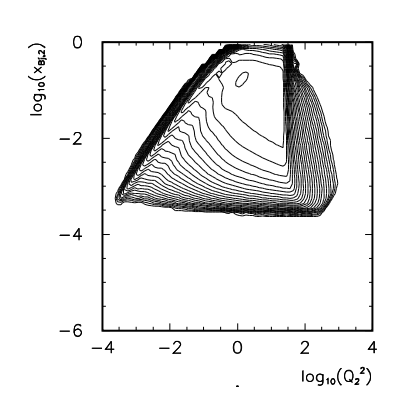


Both perturbative and nonperturbative regions



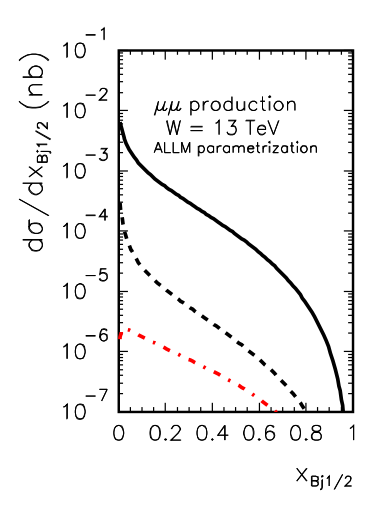
Arguments of the stucture functions, with $p_{t,pair}$ cut





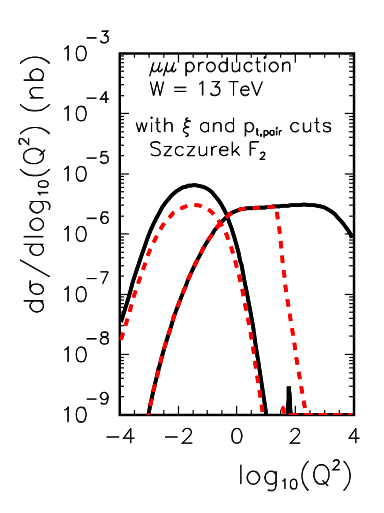
Big nonperturbative region - higher twists





Rysunek: Distribution in x_{Bj} for single dissociative process. Shown are results without (solid line) and with (dashed line) cuts on longitudinal momentum fraction ξ .

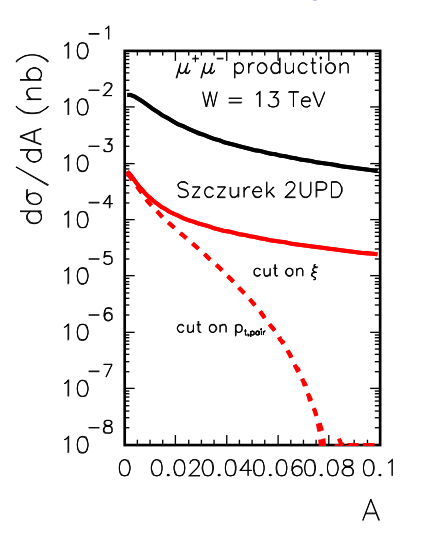
In this calculation the ALLM parametrization of F_2 structure



Rysunek: Distribution in $log_{10}(Q_i^2)$ for single dissociative process with cut on ξ and $p_{t,pair}$ (red dashed line). We show distributions for elastic (left) and inelastic (right) vertex.

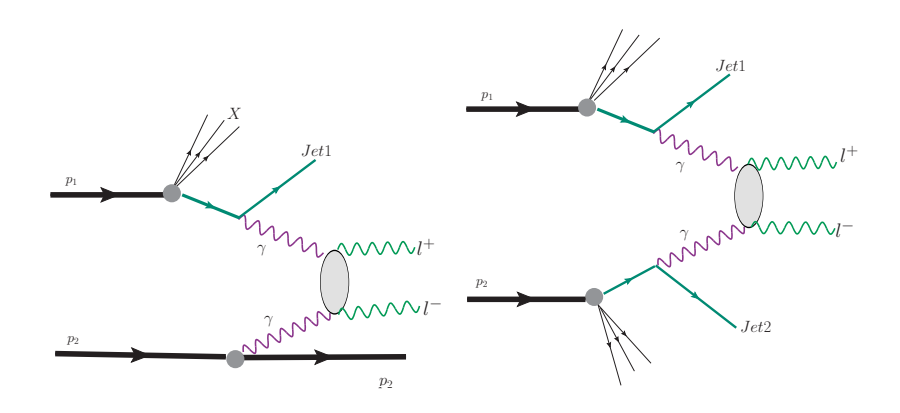
In this calculation a new Szczurek parametrization of F_2 was used.

Effect of the cuts on acoplanarity



Rysunek: Acoplanarity distribution for single dissociative contributions without any (upper black solid curve), with ξ cut (middle red solid curve) and with extra p_{ξ} and ξ 5 GeV condition

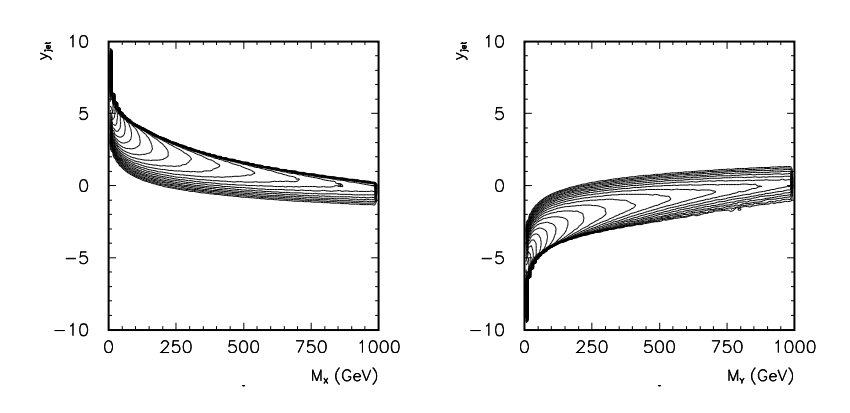
Minijets from DIS



These are only leading-order diagrams
There could be also two-jet events (more difficult).

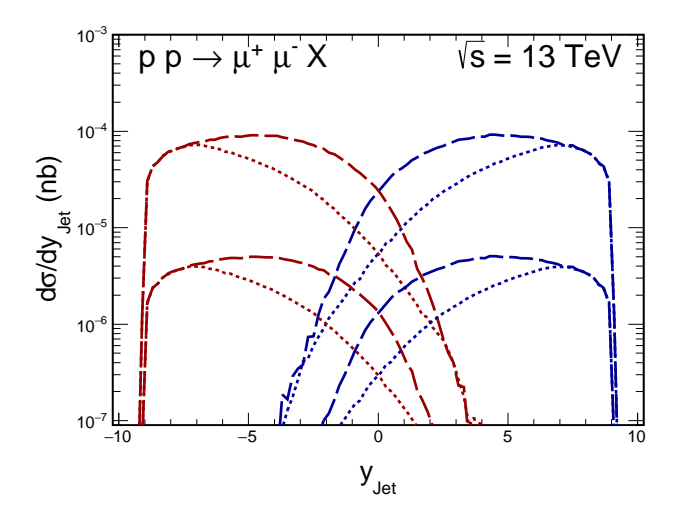


Remnant mass – y_{jet} correlations, with ξ cuts



Rysunek: $M_X - y_{jet}$ and $M_Y - y_{jet}$ correlations.

ξ_{\parallel}^{+} or ξ_{\parallel}^{-} cuts, minijets



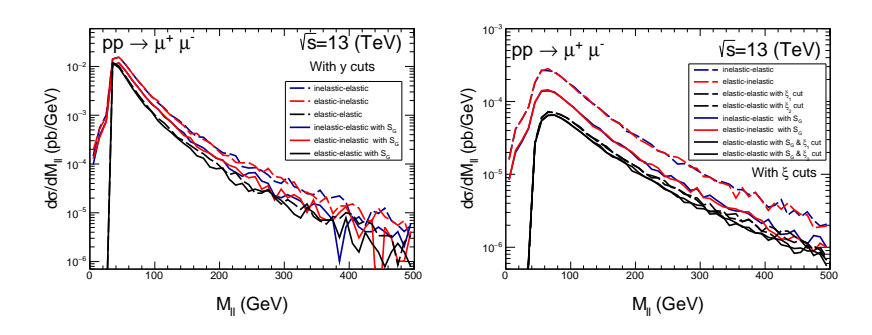
Rysunek: Distribution in rapidity of (mini)jets for inclusive case (upper curves) and for the case with cut on $\xi_{1/2}$. and $p_{t,pair} < 5$

SuperChic analysis

Tablica: Integrated cross section for $\mu^+\mu^-$ production in pb for $\sqrt{s}=13$ TeV using SuperChic program. $0.035<\xi^\pm_{ll}<0.08$. To calculate absorption effects we used model no 4 as implemented in the SuperChic generator.

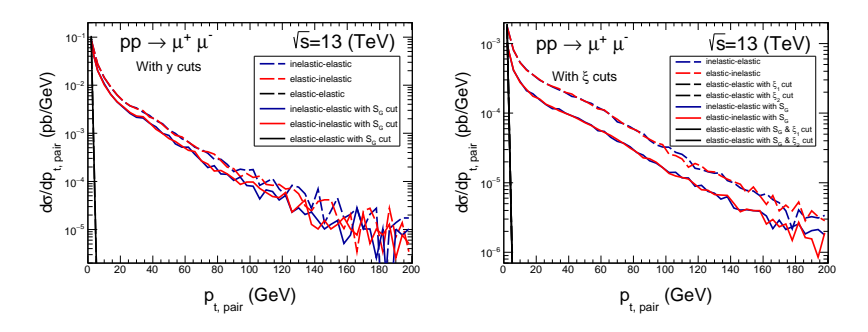
| reaction | no soft S_G | with soft S_G | $\langle S_G \rangle$ |
|---|-----------------|-----------------|-----------------------|
| $-2.5 < Y_{ } < 2.5$ | | | |
| elastic-elastic | 0.54438 | 0.50402 | 0.926 |
| inelastic-elastic | 0.89595 | 0.64283 | 0.717 |
| elastic-inelastic | 0.89587 | 0.64254 | 0.717 |
| inelastic-inelastic | 1.62859 | 0.24172 | 0.15 |
| $-2.5 < y_1, y_2 < 2.5$ in addition | | | |
| elastic-elastic | 0.42268 | 0.39355 | 0.931 |
| inelastic-elastic | 0.69241 | 0.51092 | 0.738 |
| elastic-inelastic | 0.69246 | 0.51087 | 0.738 |
| ξ cut in addition | | | |
| elastic-elastic, cut on ξ_1 | 0.00762 | 0.00675 | 0.886 |
| elastic-elastic, cut on ξ_2 | 0.00762 | 0.00675 | 0.886 |
| inelastic-elastic, cut on ξ_2 | 0.02718 | 0.01416 | 0.521 |
| elastic-inelastic, cut on ξ_1 | 0.02717 | 0.01416 | 0.521 |
| $p_{t,pair} < 5$ GeV in addition | | | |
| elastic-elastic | | | |
| inelastic-elastic, cut on ξ_2 | 0.008035 (2000) | 0.00435 | 0.541 |
| elastic-inelastic, cut on $arepsilon_1$ | 0.008056 (2000) | 0.00436 | 0.541 |

SuperChic analysis



Rysunek: Distribution in dimuon invariant mass for the different contributions considered. We consider the case without ξ cuts (left panel) and with ξ cuts (right panel).

SuperChic analysis



Rysunek: Distribution in dimuon transverse momentum for the different contributions considered. We consider the case without ξ cuts (left panel) and with ξ cuts (right panel).

SuperChic analysis, gap survival function

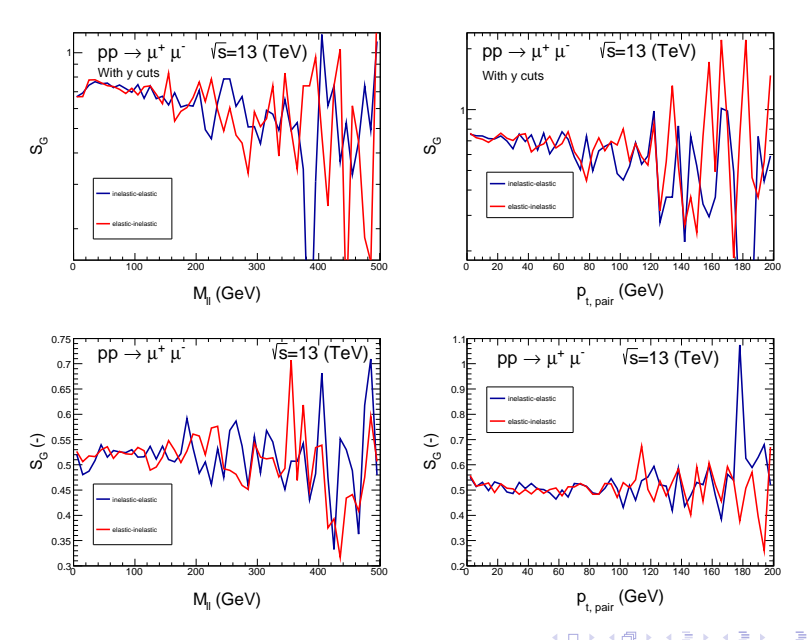
We shall show corresponding gap survival factor calculated as:

$$S_G(M_{\parallel}) = \frac{d\sigma/dM_{\parallel}|_{withSR}}{d\sigma/dM_{\parallel}|_{withoutSR}}, \qquad (10)$$

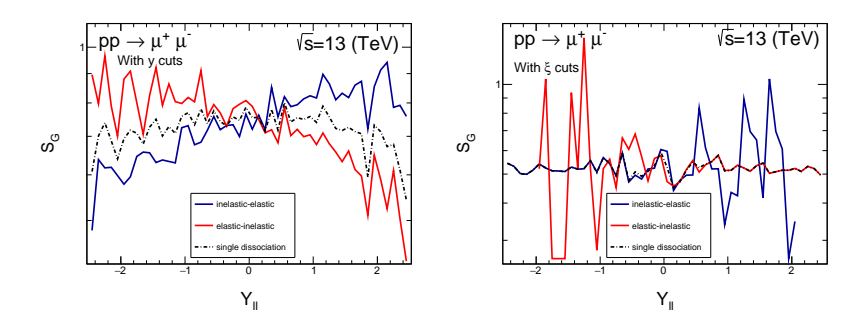
$$S_{G}(M_{II}) = \frac{d\sigma/dM_{II}|_{withSR}}{d\sigma/dM_{II}|_{withoutSR}}, \qquad (10)$$

$$S_{G}(p_{t,pair}) = \frac{d\sigma/dp_{t,pair}|_{withSR}}{d\sigma/dp_{t,pair}|_{withoutSR}}, \qquad (11)$$

SuperChic analysis, gap survival function

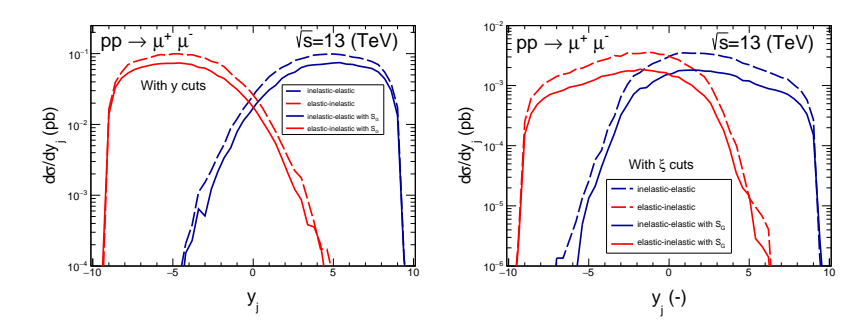


SuperChic analysis, gap survival function



Rysunek: The soft gap survival factor as a function of rapidity of the $\mu^+\mu^-$ pair for single proton dissociation. We show the result without ξ cuts (left panel) and with ξ cuts (right panel). The dash-dotted black line is effective gap survival factor for both single-dissociation components added together.

SuperChic analysis, minijet



Rysunek: Distribution in the (mini)jet rapidity for the inclusive case of no ξ cut (left panel) and when the cut on ξ is imposed (right panel) for elastic-inelastic and inelastic-elastic contributions as obtained from the SuperChic generator We show result without (dashed line) and with (solid line) soft rescattering correction.

SuperChic, gap survival factor due to jet emission

Tablica: Gap survival factor due to minijet emission. In all cases $p_{1t}, p_{2t} > 15$ GeV.

| contribution | without S_G | with S_G |
|---|---------------|------------|
| cut on Y_{II} only | | |
| elastic-inelastic | 0.76304 | 0.78756 |
| inelastic-elastic | 0.76278 | 0.78898 |
| cut on y_1 and y_2 in addition | | |
| elastic-inelastic | 0.77366 | 0.79250 |
| inelastic-elastic | 0.76926 | 0.78744 |
| cut on ξ_1 or ξ_2 in addition | | |
| elastic-inelastic | 0.48954 | 0.49986 |
| inelastic-elastic | 0.48374 | 0.49508 |
| cut on $p_{t,pair} < 5$ GeV in addition | | |
| elastic-inelastic | 0.83462 | (0.85600) |
| inelastic-elastic | 0.83462 | 0.84960 |

Conclusions

- ▶ In the present paper we have discussed dilepton production via photon-photon fusion with one forward proton which can be measured in forward detectors such as AFP for the ATLAS experiment.
- ▶ We have consider both double-elastic and single-dissociative contributions (it was argued that the contribution of double dissociation is negligible when forward proton is measured).
- ▶ In the latter case we have considered both continuum production as well as Δ^+ /resonance production. The continuum contribution is calculated for different parametrizations of the deep-inelastic structure functions from the literature.
- ▶ We have imposed conditions on ξ_1 or ξ_2 for the forward emitted protons. Several distributions have been shown and discussed.



Conclusions

- ▶ Particularly interesting is the distribution in M_{II} and the distribution in Y_{II} which has minimum at $Y_{II} \sim 0$. The minimum at $Y_{II} = 0$ is caused by the experimental condition on ξ_{II}^{\pm} related to the leading proton.
- We have also made calculations with the popular SuperChic generator and compared corresponding results to the results of our code(s). In general, the results are almost identical.
- ▶ We have calculated also soft rapidity gap survival factor as a function of M_{II} , transverse momentum of the dilepton pair, mass of the proton remnant and Y_{II} .
- ▶ No evident dependences on the variables for the single dissociation, except of distribution in *Y*_{II}. We have found different (much larger) gap survival factor for fully elastic contribution than for single proton dissociation.



Conclusions

- ➤ The soft gap survival factor for single dissociative contribution strongly depends on whether proton is measured or not. It is significantly smaller when proton is measured.
- ▶ We have also calculated gap survival factor due to mini(jet) emission by checking whether the minijet enters or not the main detector.
- ▶ The second type of the gap survival (S_{jet}) also strongly depends on whether the outgoing proton is measured or not.
 - It is about 0.8 for inclusive case (no proton measurement) and about 0.5 for the case with proton measurement in forward proton detector (with typical limited ξ value).
- ▶ small $p_{t,pair}$ → large y_{jet} → large S_{jet} .

Outlook

- ▶ In the moment only fiducial cross section was measured. In future one should measure differential distributions (better statistics, or lower $p_{l,t,min}$).
- ▶ Study large $p_{t,pair}$ region or even in bins of $p_{t,pair}$ and make a comparison bin-by-bin.
- When calculating absorptive corrections it is assumed that any interaction (independent of final state) will destroy rapidity gap or break another experimental condition on final state.
 - This has no deep justification for experimental conditions implemented for large luminosities. (pile ups). Study theoretically final state related to absorptive processes (extra pomeron exchange).
- So far only single jet topology is assumed. Single jet → double jet production for calculating rapidity gap due to jets(s) emission.
- ► There are still missing mechanisms